



Article

Cloud-Based Framework for Precision Agriculture: Optimizing Scarce Water Resources in Arid Environments amid Uncertainties

Fan Zhang ^{1,2} Peixi Tang ³, Tingting Zhou ⁴, Jiakai Liu ⁵ Feilong Li ⁶ and Baoying Shan ^{7,8,*}

¹ Yinshanbeilu Grassland Eco-Hydrology National Observation and Research Station, China Institute of Water Resources and Hydropower Research, Beijing 100038, China; zhang_fan@bjfu.edu.cn

² Jixian National Forest Ecosystem Observation and Research Station, National Ecosystem Research Network of China (CNERN), School of Soil and Water Conservation, Beijing Forestry University, Beijing 100083, China

³ School of Water Conservancy & Civil Engineering, Northeast Agricultural University, Harbin 150030, China; peixitang0328@163.com

⁴ State Key Laboratory of Environmental Criteria and Risk Assessment, Chinese Research Academy of Environmental Sciences, Beijing 100012, China; zhoutt@craes.org.cn

⁵ School of Ecology and Nature Conservation, Beijing Forestry University, Beijing 100083, China; jkliu@bjfu.edu.cn

⁶ Guangdong Provincial Key Laboratory of Water Quality Improvement and Ecological Restoration for Watersheds, School of Ecology, Environment and Resources, Guangdong University of Technology, Guangzhou 510006, China; fl_li@gdut.edu.cn

⁷ Research Unit Knowledge-Based System, Ghent University, 9000 Ghent, Belgium

⁸ Hydro-Climatic Extremes Lab, Ghent University, 9000 Ghent, Belgium

* Correspondence: baoying.shan@ugent.be

Abstract: In arid agriculture, the effective allocation of scarce water resources and the assessment of irrigation shortage risks are critical water management practices. However, these practices are faced with inherent and unignorable uncertainties affecting multiple variables. This study aims to model the typical uncertainties in these practices and understand how they impact the allocation of scarce water resources. We advocate for a nuanced consideration of variable characteristics and data availability, variation, and distribution when choosing uncertainty representation methods. We proposed a comprehensive framework that integrates the cloud model to delineate scenarios marked by subjective vagueness, such as “high” or “low” prices. Simultaneously, the stochastic method was used for modeling meteorological and hydrological variables, notably precipitation and crop evapotranspiration. Additionally, to navigate subjectivity and imprecise judgment in standards classification, this framework contains a cloud-model-based assessment method tailored for evaluating irrigation shortage risks. The proposed framework was applied to a real-world agricultural water management problem in Liangzhou County, northwest China. The results underscored the efficacy of the cloud model in representing subjective vagueness, both in the optimization process and the subsequent assessment. Notably, our findings revealed that price predominantly influences net benefits, and that precipitation and crop evapotranspiration emerge as decisive factors in determining optimal irrigation schemes. Moreover, the identification of high water storage risks for maize in the Yongchang and Jinyang districts serves as a reminder for local water managers of the need to prioritize these areas. By adeptly modeling multiple uncertainties, our framework equips water managers with tools to discern sensitive variables. We suggest that enhanced precipitation and evapotranspiration forecasts could be a promising way to narrow the uncertainties.



Citation: Zhang, F.; Tang, P.; Zhou, T.; Liu, J.; Li, F.; Shan, B. Cloud-Based Framework for Precision Agriculture: Optimizing Scarce Water Resources in Arid Environments amid Uncertainties. *Agronomy* **2024**, *14*, 45. <https://doi.org/10.3390/agronomy14010045>

Academic Editor: Robert J. Lascano

Received: 3 December 2023

Revised: 22 December 2023

Accepted: 22 December 2023

Published: 22 December 2023



Copyright: © 2023 by the authors. Licensee MDPI, Basel, Switzerland. This article is an open access article distributed under the terms and conditions of the Creative Commons Attribution (CC BY) license (<https://creativecommons.org/licenses/by/4.0/>).

Keywords: cloud model; uncertainty; agricultural water optimization; water storage risk assessment; precision agriculture

1. Introduction

The burgeoning global population and the rapid pace of economic development underscore the need for the sustainable advancement of agriculture [1–3]. Irrigation is one

of the critical practices deployed to enhance production, strengthen food security and amplify economic returns by up to 400% in arid agriculture [4–6]. Unfortunately, arid regions face the pervasive threat of water scarcity, jeopardizing crop growth and agricultural production worldwide [7,8]. The effective allocation of limited water resources for irrigation is essential, particularly in agriculturally dominated developing regions [9,10]. In practice, the management of water resources in arid agriculture confronts inherent uncertainties arising from diverse aspects [11,12], such as climate conditions (e.g., variable precipitation), management strategies (e.g., price volatility), and the risk tolerance of policymakers. These uncertainties can compromise the applicability, reliability, and robustness of water management practices, potentially providing inaccurate references for policymakers [12,13].

Various mathematical methods, such as interval, fuzzy, random, and their combinations and extensions have been proposed and applied to the representation of uncertainty in previous studies [11,14–18]. However, inconsistencies in the representation of the same variable across different studies, coupled with a lack of clear criteria for method selection, have created confusion. For example, Ma et al. [19] considered available water supply as an interval number while Wang et al. [20] represented water availability as an inexact fuzzy number. Precipitation was represented as a random number in [21] while it was described as a fuzzy-interval set in [22]. This necessitates a more thorough examination of uncertainty representation methods.

The selection of an uncertainty representation method should be contingent upon the intrinsic features of the variable and data characteristics, such as availability, variation, and distribution [23]. Randomness, for example, proves effective in addressing uncertainty related to climate variables like precipitation [24] owing to the availability of long-term measured data and natural mechanisms. Conversely, highly vague variables, such as high crop prices or risk levels, are better suited to methods beyond randomness [25]. The subjective nature of terms like “high” makes fuzzy theory a common choice [16,26,27], but this theory struggles to capture the varying and vague membership degrees assigned by different individuals. The cloud model [28], as an advancement in membership function, exhibits potential in capturing complex variability in uncertainty-based evaluation [29–33], knowledge representation [34,35] and data mining [36]. The cloud model assumes that the membership degree between a real number and a concept is not fixed, but a random number [37], which aligns more closely with real-world scenarios.

Our objectives are to model the uncertainties both in optimizing irrigation water resources and evaluating the risks faced by arid regions. Building on the advantages of the cloud model, we propose a cloud-based framework for precision agriculture in this study (see Figure 1). The primary focus is on optimizing scarce water resources and assessing water shortage risks in arid environments amidst multiple uncertainties. Specifically, the cloud model and stochastic method are integrated into the optimization model based on the features of the variable itself and the available data. Additionally, a cloud model-based evaluation method is developed to elucidate uncertainties in classifying risk levels and evaluating multiple factors. The Shiyang River Basin in Northwestern China serves as a crucial case study. The study seeks to understand how uncertainties impact the allocation of scarce water resources. The proposed framework is poised to assist local decision-makers in developing effective and sustainable agricultural allocation schemes, with potential implications for other arid regions worldwide.

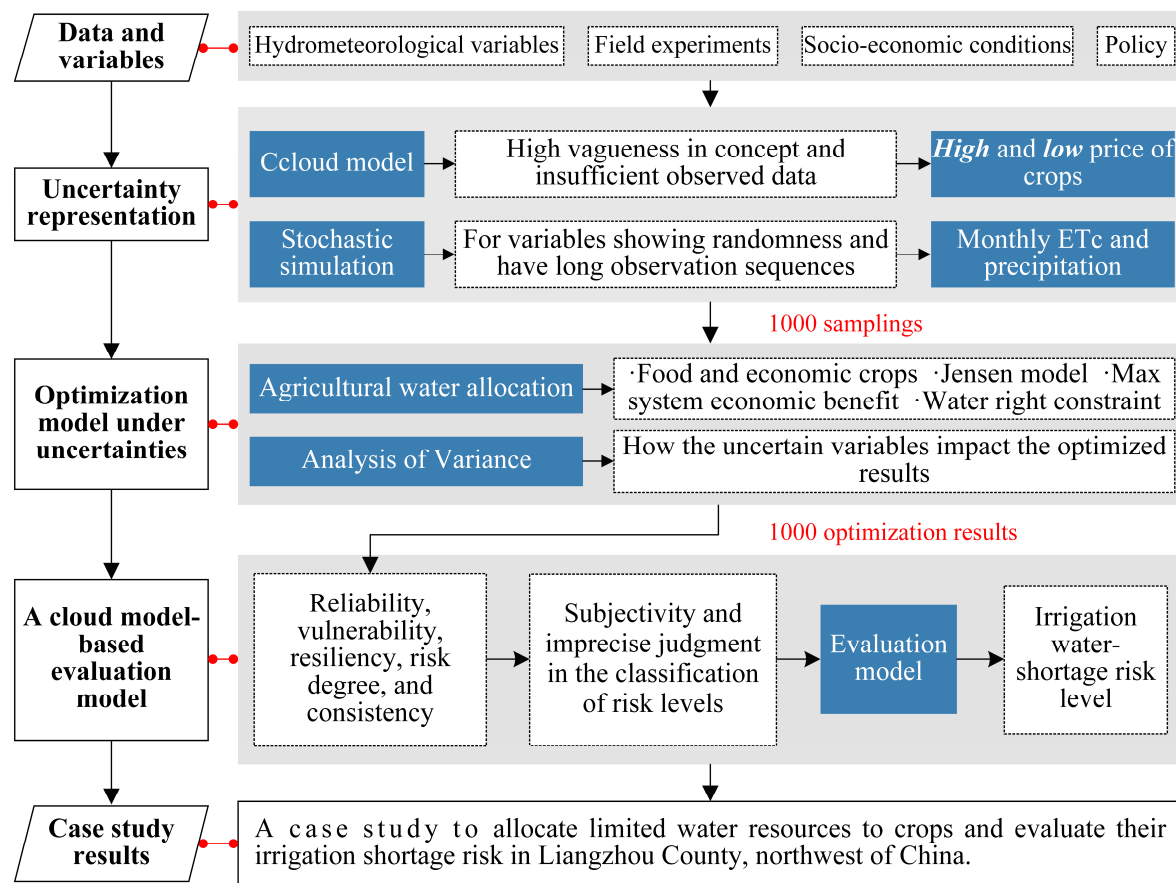


Figure 1. Framework of this study. This study makes use of hydrometeorological, field, socioeconomic, and policy data. We consider multiple uncertain variables represented by the cloud model and the stochastic method. The optimization model was built to allocate the limited water resources for the maximum economic benefit. We further evaluated the irrigation shortage risk. We applied the above framework to a case study in a typical arid region in China.

2. Materials and Methods

2.1. Optimization Model

With the aim of efficiently allocating limited agricultural water resources to different crops each month in order to maximize economic benefits, we built an agricultural water optimization model. The objective of this model is to achieve the highest possible system net benefit across the entire research area. We divide crops into food crops (e.g., maize and wheat) and economic crops (e.g., vegetables). For food crops, the relationship between crop yields and water consumption is quantified using the Jensen model [38]. Due to the limited availability of field experiments and variations in the types of economic crops, their irrigation–benefit relationship is simplified as linear. The objective function is defined as follows:

$$\max F = \sum_{k=1}^K \sum_{i=1}^I CP_i A_{ki} Y_{max,i} \prod_{t=1}^T \left(\frac{ET_{kit}}{ET_{c,it}} \right)^{\lambda_{it}} + \sum_{k=1}^K V_k A_{k3} W_{k3} - \left(C_0 + \sum_{k=1}^K C_k \sum_{i=1}^I \sum_{t=1}^T W_{kit} \right) \quad (1)$$

where F is the system's net economic benefit (CNY, Chinese Yuan), which is equal to the benefit of food crops plus the benefit of economic crops, then minus the cost; k is the study subarea; i is the food crop; t is the growth month; CP_i is the price of food crop i (CNY/kg); A_{ki} is the planting area of food crop i in subarea k (ha); $Y_{max,i}$ is the maximum crop yield under full irrigation of food crop i (kg/ha); ET_{kit} is the actual evapotranspiration of crop i during month t , calculated by the soil–water balance formula (mm); $ET_{c,it}$ is the crop

evapotranspiration (crop water requirements, also the maximum evapotranspiration) of food crop i during month t (mm); V_k is the net benefit coefficient in subarea k per unit of water allocated (CNY/m³); A_{k3} is the planting area of all economic crops in subarea k (ha); W_{k3} is the decision variable denoting the irrigation amount of economic crops in subarea k (mm); C_0 is the planting cost, including the cost of seeds, fertilizers, pesticides, mechanical operations, etc. (CNY/ha); C_k is the cost of a unit of irrigated water in subarea k (CNY/m³); W_{kit} is the decision variable denoting the irrigation amount of food crop i during month t in subarea k (mm).

The objective function is subjected to several constraints including soil–water balance, water availability, and irrigation water demand.

1. Soil–water balance constraint

$$\text{ET}_{kit} = W_{kit} + \text{EP}_t + \Delta S_{kit} - K_{kit}, \forall k, i, t \quad (2)$$

where EP_t is the effective precipitation during month t (mm). EP_t can be calculated by the effective coefficient method [39], $\text{EP}_t = \mu P_t$, where μ is the effective coefficient and P_t is the precipitation during month t ; ΔS_{kit} is the change of soil water content (mm); K_{kit} is the drainage of water below the root zone to the groundwater (mm).

2. Water availability

$$\left(\sum_{i=1}^I \sum_{t=1}^K A_k W_{kit} + A_{k3} W_{k3} \right) \leq \beta_k \eta_k \text{WR}_k, \forall k \quad (3)$$

where β_k is the proportion of irrigation water during crop growth in subarea k ; η_k is the coefficient of irrigation water use in subarea k ; WR_k is the agricultural water availability in subarea k (m³). For every subarea, the total amount of irrigation needed does not exceed the amount of disposable water.

3. Irrigation water demand constraint

$$\text{ET}_{\min,it} \leq \text{ET}_{kit} \leq \text{ET}_{c,it}, \forall k, i, t \quad (4)$$

$$W_k^{\min} \leq W_{k3} \leq W_k^{\max} \quad (5)$$

where $\text{ET}_{\min,it}$ is the minimum water demand (mm); W_k^{\min} and W_k^{\max} are the minimum and maximum irrigation demands for economic crops in subarea k (mm).

We emphasize that this water resource optimization model is highly simplified. It focuses on the impacts of water resources on the crop yield and economic benefits in the arid regions, while other possible impacted factors like soil acidity and salinity are not included in this study.

2.2. Uncertainties in the Optimization Model

In the context of agricultural water management in water-limited regions, precipitation is the key input of the available water resources. Crop evapotranspiration is driven by crop type and climate variables, such as radiation and temperature. Precipitation and crop evapotranspiration vary across years with large variations. Additionally, crop prices directly impact overall agricultural benefits, presenting a crucial factor for farmers. Given their significance and temporal variability, this study emphasizes the uncertainty associated with precipitation, crop evapotranspiration, and crop prices.

Among these variables, precipitation and crop evapotranspiration exhibit a degree of randomness and often have long-term observation time series [24]. Consequently, they are appropriately represented using stochastic methods. Specifically, $\text{ET}_{c,it}$ is fitted using a Gaussian distribution [40], while P_t follows a three-parameters gamma distribution (Pearson type III, abbreviated to P-III) due to the typically forward-skewed nature of precipitation distribution. N-groups of P_t and $\text{ET}_{c,it}$ are generated based on simulated distribution functions, and these groups are then used as inputs for the optimization model.

Considering crop prices under two market conditions—“high” and “low”—poses a distinct challenge due to the subjective nature of language terms. Leveraging the advancements of the cloud model over the traditional fuzzy method, this study applies the cloud mode (see Figure 2) to represent uncertainties in the scarce water optimization process. Definition and calculation details of cloud model are shown in the Appendix A. The proposed framework involves the following steps (see Figure 3):

1. Determine uncertain variables suitable to be represented by the cloud model, assuming there are I factors;
2. Collect measurement or experimental data series $\{X_{i1}, X_{i2}, \dots, X_{iD}\}$ for i -th variable, assuming there are D numbers for i -th variable;
3. Calculate the variable cloud C_i using a backward generator algorithm (details shown in Appendix A). The three numerical characteristics of cloud C_i for i -th variable are Ex_i , En_i and He_i ;
4. Generate cloud drops. Given a sampling number N , generate N -group cloud drops $Drop(x_{in}, \mu_{in})$ based on $C_i = (Ex_i, En_i, He_i)$ using a forward generator algorithm (Equation (6)). More details are shown in Appendix A.

$$\begin{cases} En'_{in} = \text{NORM}(En_i, He_i^2) \\ x_{in} = \text{NORM}(Ex_i, En'_{in}) \\ \mu_{in} = \exp\left(-\frac{(x_{in}-Ex_i)^2}{2(En'_{in})^2}\right) \end{cases} \quad (6)$$

where $n = 1, 2, \dots, N$, En'_{in} is a normally distributed number with expectation En_i and variance He_i^2 and x_{in} is a normally distributed random number with expectation Ex_i and variance En'_{in} .

5. Integration into the optimization model. Bring the N -group of cloud drops (x_{in}, μ_{in}) into the optimization model separately and run optimization model N times.

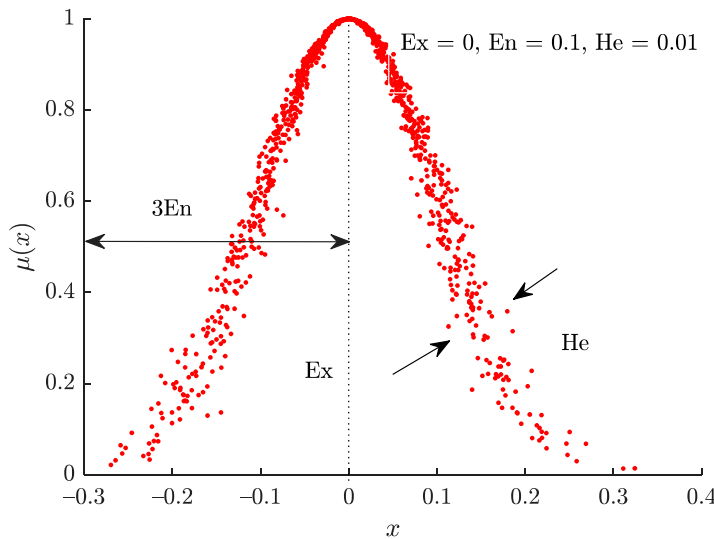


Figure 2. An example of a cloud model and its expected value (Ex), entropy (En), and hyper entropy (He). $\mu(x)$ is the certainty degree of a number x belonging to a concept.

Furthermore, assessing the impact of uncertainties in inputs on the optimization results is crucial for providing decision-makers with insights into the significance and sensitivity of each uncertain variable. In this study, the analysis of variance is used to distinguish uncertainties arising from each uncertain variable and their interaction [41,42].

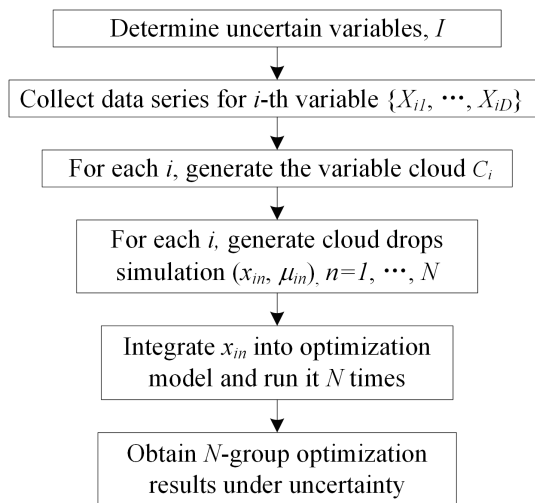


Figure 3. The flow chart for applying the cloud model for uncertainty representation and combining it with the optimization model. The detailed description is shown in Section 2.2.

2.3. Irrigation Water Shortage Risk Evaluation

To further understand the system's water shortage risk after the optimized schemes are applied in practice, we conducted a risk evaluation. This evaluation, aiming for objectivity and credibility, considers not only vulnerability (shortage amount) but also irrigation reliability (probability without shortage risk), consistency (dynamic response between water supply and demand), recoverability (ability to return to normal from a crashed state), and the degree of scheme dispersion (dispersion of water shortage). Five factors are used to comprehensively characterize water resource system behavior. Refer to references [40,43,44] for detailed definitions and calculations of these factors. Each evaluation factor is categorized into five risk levels, outlined in Table 1.

Table 1. Evaluation factors are divided into five risk levels: the low risk level (I), lower middle risk level (II), middle risk level (III), upper middle risk level (IV), and high-risk level (V). R₁ to R₅ represent the values of five factors, $0 \leq R \leq 1$.

Risk Level	Reliability	Vulnerability	Resiliency	Consistency Index	Risk Degree
Low risk level (I)	$R_1 \leq 0.2$	$R_2 \leq 0.2$	$R_3 > 0.8$	$R_4 > 0.8$	$R_5 \leq 0.2$
Lower middle risk level (II)	$0.2 < R_1 \leq 0.4$	$0.2 < R_2 \leq 0.4$	$0.6 < R_3 \leq 0.8$	$0.6 < R_4 \leq 0.8$	$0.2 < R_5 \leq 0.4$
Middle risk level (III)	$0.4 < R_1 \leq 0.6$	$0.4 < R_2 \leq 0.6$	$0.4 < R_3 \leq 0.6$	$0.4 < R_4 \leq 0.6$	$0.4 < R_5 \leq 0.6$
Upper middle risk level (IV)	$0.6 < R_1 \leq 0.8$	$0.6 < R_2 \leq 0.8$	$0.2 < R_3 \leq 0.4$	$0.2 < R_4 \leq 0.4$	$0.6 < R_5 \leq 0.8$
High risk level (V)	$R_1 > 0.8$	$R_2 > 0.8$	$R_3 \leq 0.2$	$R_4 \leq 0.2$	$R_5 > 0.8$

What is more, a cloud model-based evaluation method is proposed to represent uncertainties of level division and multiple evaluation sets, which is caused by subjectivity and imprecise judgment. The steps are listed as follows (see Figure 4):

1. Select the evaluation index factor and obtain classification standards from experts. Assume there are I indexes divided into J levels;
2. Generate the classification cloud C_{ij} for each level of each index factor using a backward generator algorithm (see Equation (A3) in Appendix A). The characteristic parameters of cloud C_{ij} for the i -th index factor at the j -th level are Ex_{ij} , En_{ij} , and He_{ij} ;
3. Assume there are K sets of samples for each i to be evaluated and calculate the value of the i -th index factor m_{ik} ;
4. For each set, calculate the certainty degree μ_{ijk} of m_{ik} in the j -th C_{ij} for every j as in Equation (7).

$$\begin{cases} \mu_t = \exp\left(-\frac{(m_{ik}-Ex_{ij})^2}{2(En'_t)^2}\right), En'_t \sim N(En_{ij}, He_{ij}^2), t = 1, 2, \dots, T, \forall j \\ \mu_{ijk} = \frac{1}{T} \sum_{t=1}^T \mu_t \end{cases} \quad (7)$$

where En'_t is a normally distributed random number with expectation En_{ij} and variance He_{ij}^2 and μ_t is the degree of certainty that the index value m_{ik} members to j -th cloud C_{ij} . Due to the randomness of the cloud model, the certainty degree μ_t is not fixed, changing with each calculation. So repeatedly calculate μ_t T times and μ_{ijk} is the average of μ_t ;

5. For each k , repeat step 4. The certainty degree of the i -th index factor to the j -th level is calculated by the average of μ_{ijk} .

$$\mu_{ij} = \sum_{k=1}^K \mu_{ijk} \quad (8)$$

6. Normalization. In this study, the normalized certainty degree is called the relative membership degree, calculated as:

$$\mu'_{ij} = \mu_{ij} / \sum_{j=1}^J \mu_{ij} \quad (9)$$

where μ'_{ij} is the relative membership degree, $0 \leq \mu'_{ij} \leq 1$;

7. Repeat steps 3–6 for each evaluation factor I ;
8. Obtain the comprehensive evaluation level. The level where the maximum W_j (Equation (10)) is located is the final evaluation level.

$$W_j = \sum_{i=1}^I \omega_i \mu'_{ij}, \forall j \quad (10)$$

where ω_i is the weight of the i -th evaluation index.

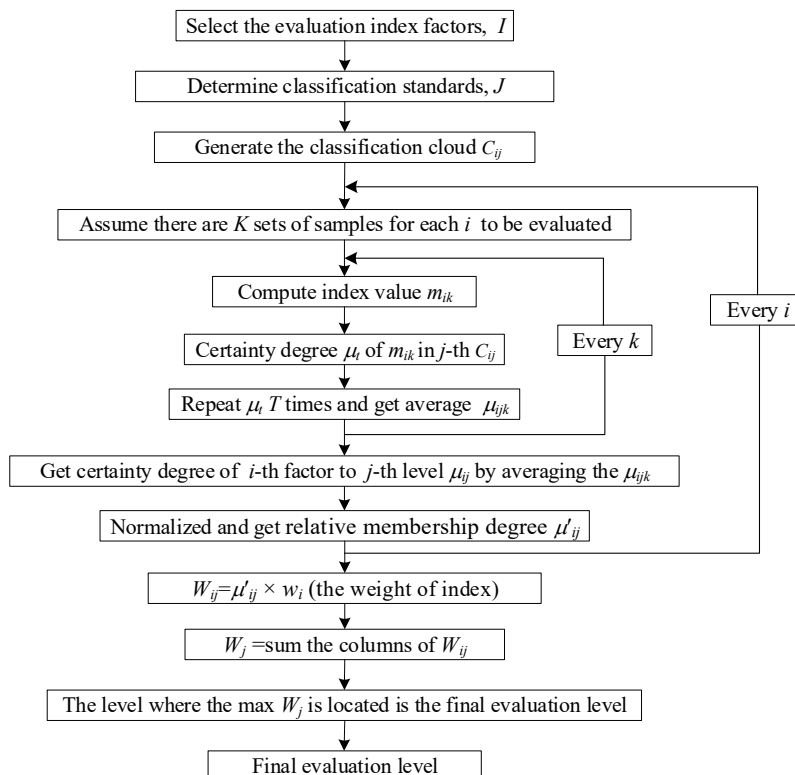


Figure 4. The flow chart for applying the cloud model for the evaluation method amid uncertainty. The detailed description is shown in Section 2.3.

3. Case Study

3.1. Study Area

Our case study focuses on a typical arid region, specifically Liangzhou County, located in the middle of the Shiyang River Basin ($101^{\circ}41'$ – $104^{\circ}16'$ E and $36^{\circ}29'$ – $39^{\circ}27'$ N), China, shown in Figure 5. Liangzhou County experiences a typical inland arid climate, with an average annual precipitation of 158 mm and potential evaporation reaching 2021 mm. Agriculture is the primary industry in the Shiyang River Basin; heavily reliant on irrigation. However, unregulated water use has led to ecological challenges downstream, including a decline in groundwater levels, lake drying, and increased desertification.

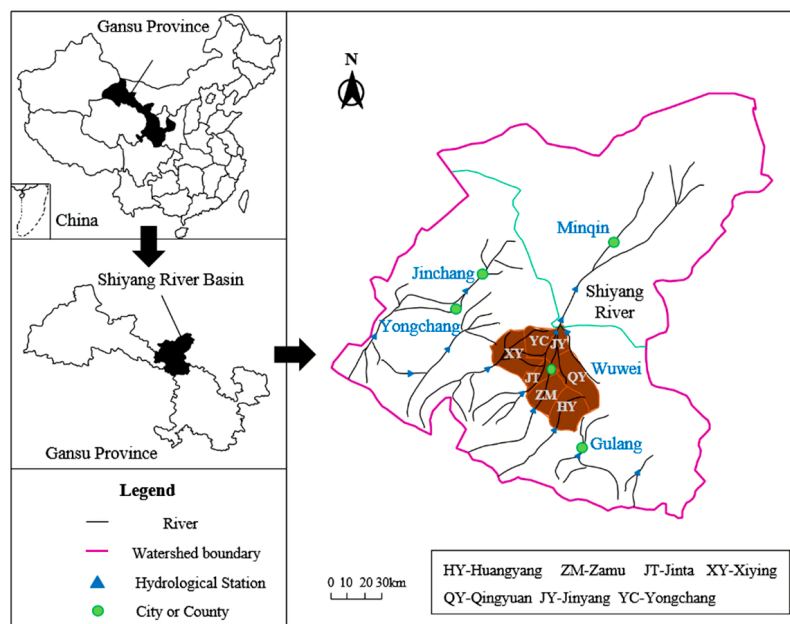


Figure 5. Study area. The seven irrigation districts (XY, ZM, HY, JT, QY, YC, and JY) are in the middle of the Shiyang River Basin, located in an inland area in the northwest of China. We allocate the scarce water resource to the Xiying (XY), Zamu (ZM), Huangyang (HY), Jinta (JT), Qingyuan (QY), Yongchang (YC), and Jinyang (JY) irrigation districts.

Liangzhou County stands out as the highest water consumer among the six major counties in the Shiyang River Basin, accounting for 41% of the total water consumption in 2016, reaching 940 million m³. The agricultural sector, constituting 81% of the economy, is the primary user of water in the Liangzhou District. Implementing a more efficient agricultural irrigation scheme is essential for rational water use and achieving maximum system benefits. The study narrows its focus to seven main irrigation districts in Liangzhou County: the Xiying (XY), Zamu (ZM), Huangyang (HY), Jinta (JT), Qingyuan (QY), Yongchang (YC), and Jinyang (JY) irrigation districts. Among these, QY, YC, and JY rely on groundwater for irrigation, while the others are predominantly irrigated by river water. Maize (growing time from April to September) and wheat (growing time from March to July) are the main crops in Liangzhou County, constituting over 60% of the total planting area in the XY, ZM, HY, JT, and YC irrigation areas. Other crops, collectively referred to as economic crops, include oilseeds (flax, rapeseed, oil sunflower, etc.), sugar beet, medicinal materials, vegetables, melons, sunflower, sweet sorghum, green fodder, potatoes, beer barley, and beans. These crops, while occupying smaller proportions, enjoy a stable net benefit coefficient (V_k in Equation (1)).

Focusing on the seven irrigation districts and main crops in Liangzhou County, we allocate limited water to maize and wheat each month and the economic crops during the entire growing season in each county. In total, there are $7 \times (5 + 6) + 7 = 84$ decision variables. Four marketing scenarios were set up: low-price wheat–low-price maize (S1),

high-price wheat–low-price maize (S2), low-price wheat–high-price maize (S3), and high-price wheat–high-price maize (S4).

3.2. Data

The growing period of wheat and maize is from March to July and from April to September, respectively. Monthly crop evapotranspiration (crop water requirement) was calculated by the FAO 56 Penman–Monteith method [45]. The meteorological data from 1956 to 2017 were obtained from the National Meteorological Science Data Center (<http://data.cma.cn/> (accessed on 30 November 2019)), including temperature, precipitation, radiation, sunshine, wind speed, etc.

The market prices of wheat and maize (From 2009 to 2020) were obtained from the public business information service website of the Ministry of Commerce (<http://cif.mofcom.gov.cn> (accessed on 3 March 2021)). Each crop's price was separated into two sets by median value for building cloud models.

The local government has formulated a strict water rights allocation plan for each irrigation district to control the total water consumption. The amount of irrigation cannot exceed the agricultural water rights for each irrigation district. Therefore, agricultural water rights were used as the water availability constraint.

Water sensitivity indexes for different growth months of the Jensen model were obtained from Zhang et al. [46]. Other data, such as water price, the planting area of crops, irrigation coefficients, planting cost, agricultural water rights, etc., were obtained from field research.

4. Results and Discussion

4.1. Water Resources Allocation Schemes

A total of 1000 samplings of “high” and “low” prices for wheat and maize, represented by cloud models, are depicted in Figure 6. The certainty degree regarding whether a price is perceived as “high” or “low” varies among individuals for each price point. There is an intersection of samplings (cloud drops) between “high” and “low” prices for each crop, aligning with diverse human perspectives. For example, individuals may categorize a specific price as either “high” or “low” based on their interpretation. Simulated distribution results demonstrate the effectiveness of using normal and P-III distributions to describe precipitation and crop evapotranspiration. Detailed results are available in the Supplementary Figure S2.

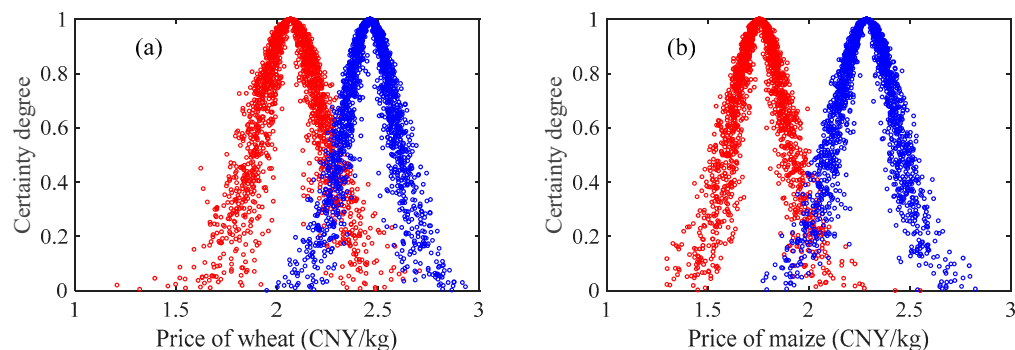


Figure 6. Plotted are the certainty degree for wheat (a) and for maize (b) as a function of their respective price, shown in “blue” for high and in “red” for low.

Then, optimization results under multiple uncertainties are obtained, including system net benefits (Figure 7), monthly optimized irrigation schemes of wheat and maize, and the whole-growth-period irrigation scheme for economic crops.

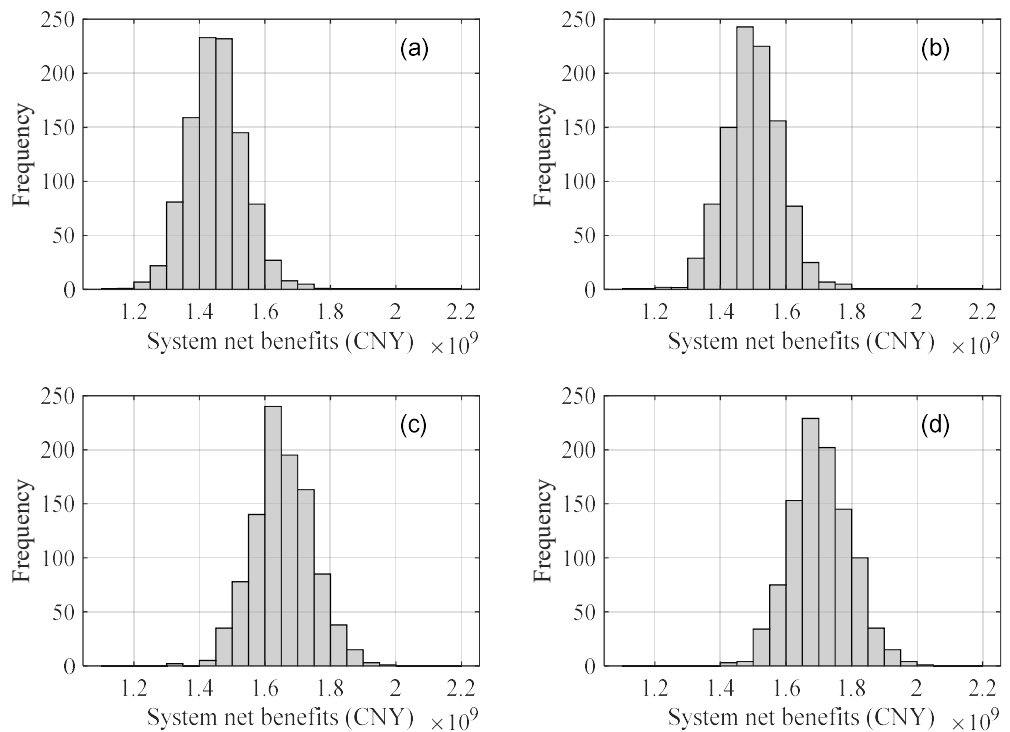


Figure 7. Frequency of system net benefits in four scenarios: (a–d) represent four scenarios of low prices of wheat and maize, high-price wheat–low-price maize, low-price wheat–high-price maize, and high prices of wheat and maize, respectively.

The optimization model not only shows the range of system net benefits but also provides the possibility of achieving an optimized benefit under the influence of uncertain variables. Taking S1 (with low prices of wheat and maize) as an example, the probability of system net benefits between $[1.27, 1.65] \times 10^9$ CNY reaches 97%, and the probability between $[1.38, 1.55] \times 10^9$ CNY reaches 69% in Liangzhou County. For scenarios 1 to 4, the net benefits have an increasing trend. Their median values are 1.45, 1.50, 1.65, and 1.70 (10^9 CNY) for S1 to S4, respectively. This is because of the tendency of higher crop prices in the four market scenarios. The high price of maize could contribute more to the total benefits than wheat as the benefits of S3 (low-price wheat–high-price maize) is higher than S2 (high-price wheat–low-price maize).

Economic crops occupy an advantageous position in the water-allocation process. As shown in Figure 8, the water supply satisfaction of economic crops is always larger or equal to that of food crops for all districts. Economic crops' water requirements are met 100% in five of the seven districts. This is because, compared with maize and wheat, economic crops can generally gain higher benefits under the same amount of irrigation water. Therefore, water managers should meet the water demands of economic crops first to achieve higher system-wide economic benefits. Between the two food crops, the water supply satisfaction of maize is higher than that of wheat, which may partly contribute to the lower total water demand of maize (with mean evapotranspiration values of 640 mm and 522 mm for wheat and maize) and more precipitation during maize's growing period (with mean precipitation of 82 mm and 144 mm during the growing period of wheat and maize). QY has the lowest water supply satisfaction among the seven irrigation districts, followed by HY. JT has the highest water supply satisfaction.

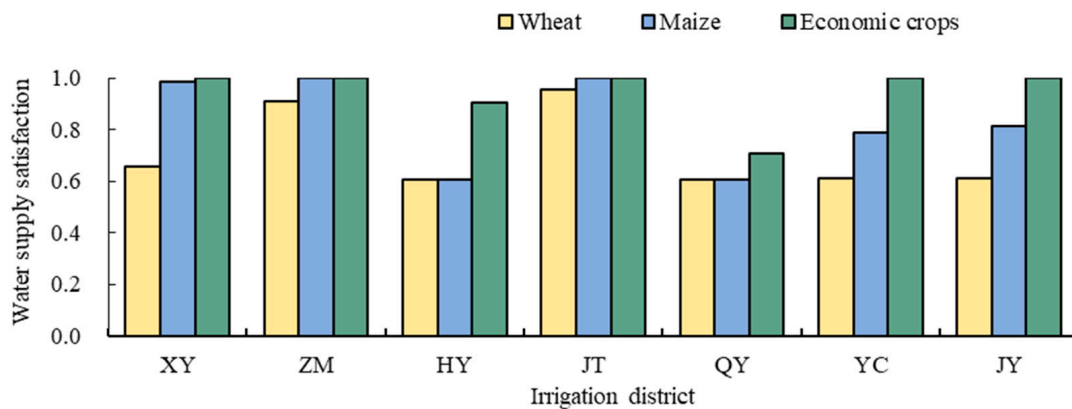


Figure 8. Water supply satisfaction after optimization during the whole growing period for each irrigation district and each crop.

To analyze the irrigation allocation for each month, taking the XY irrigation area under scenario 1 as an example, Figure 9 shows the frequency of optimized irrigation schemes under multiple uncertainties. The irrigation allocation of economic crops is fixed in the XY district, always at the maximum (630 mm during the whole period). For maize and wheat, the clear distribution of optimized allocation can be obtained instead of simply obtaining the upper and lower bounds. So, the proposed optimization model can provide water managers with more specific and useful information. For example, the lower and upper bounds of water allocation in April for maize are 0 and 30.4 mm. A range this large will cause confusion among water managers. But thanks to the specific distribution of the optimization results, the 5% and 95% quantiles for maize in April are 7.9 mm and 24.6 mm. The optimal irrigation scheme has a 90% probability of {7.9, 24.6} mm. Only a few allocation schemes are at their extreme positions. Water managers can choose an allocation scheme based on local irrigation guarantee rates.

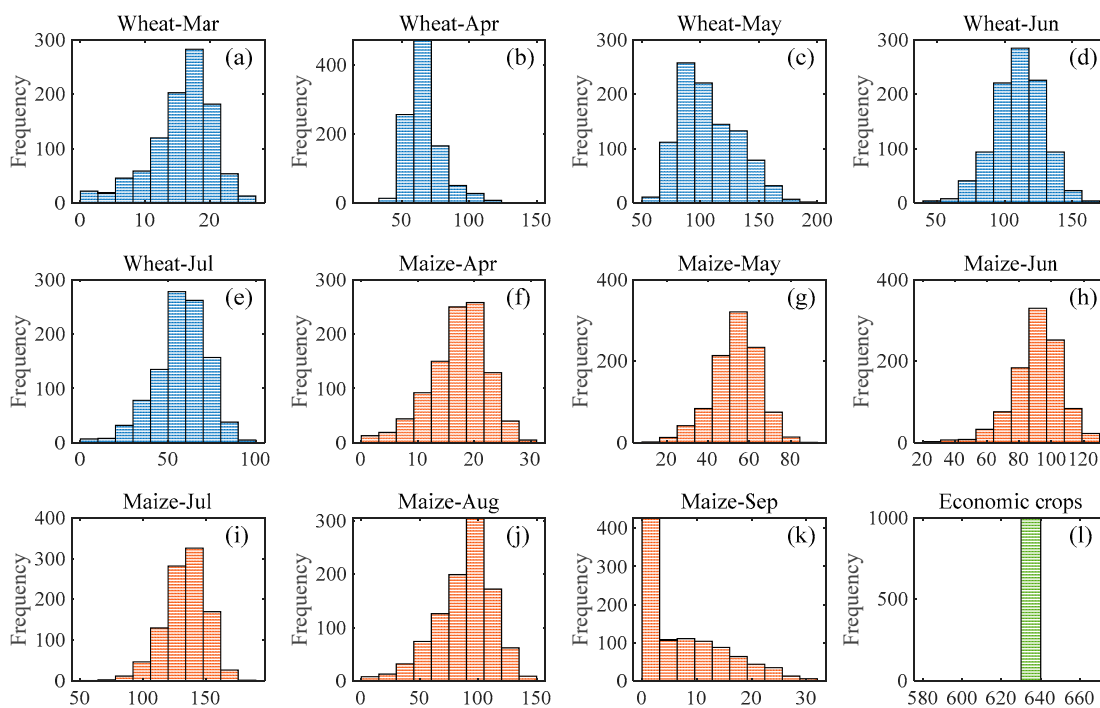


Figure 9. Frequency of optimized irrigation amounts for each crop, taking the XY district and scenario 1 as an example: (a–e) are for wheat, (f–k) are for maize, and (l) is for economic crops.

4.2. Contribution of Uncertain Variables to the Variation in Results

The optimized allocation schemes and objectives exhibit considerable variation, stemming from the uncertainty inherent in input variables. To ascertain the primary contributor to this variation, the ANOVA method was applied to quantify the influence of crop evapotranspiration, precipitation, crop price, and their intersection on the overall ensemble variation in both the optimized allocation schemes and the objectives.

Precipitation and crop evapotranspiration uncertainties predominantly drive the variation in optimized irrigation schemes, with crop price making a negligible contribution. The detailed contributions in the four scenarios are shown in Figure 10. In 59 out of 77 cases, uncertainty in precipitation emerges as the principal driver of variation in optimized water allocation schemes, particularly notable for maize in the HY, QY, YC, and JY irrigation districts. In the remaining 18 cases, uncertainty in crop evapotranspiration plays a key role, such as in wheat from April to July in the HY, JT, QY, YC, and JY districts, as well as maize in July in the XY, ZM, and JT districts. The uncertainty in price and the inter-section term contribute little to the variation in optimized water allocation schemes. The four price scenarios produce similar results, which also reveals that changes in crop prices hardly impact the optimized water allocation schemes.

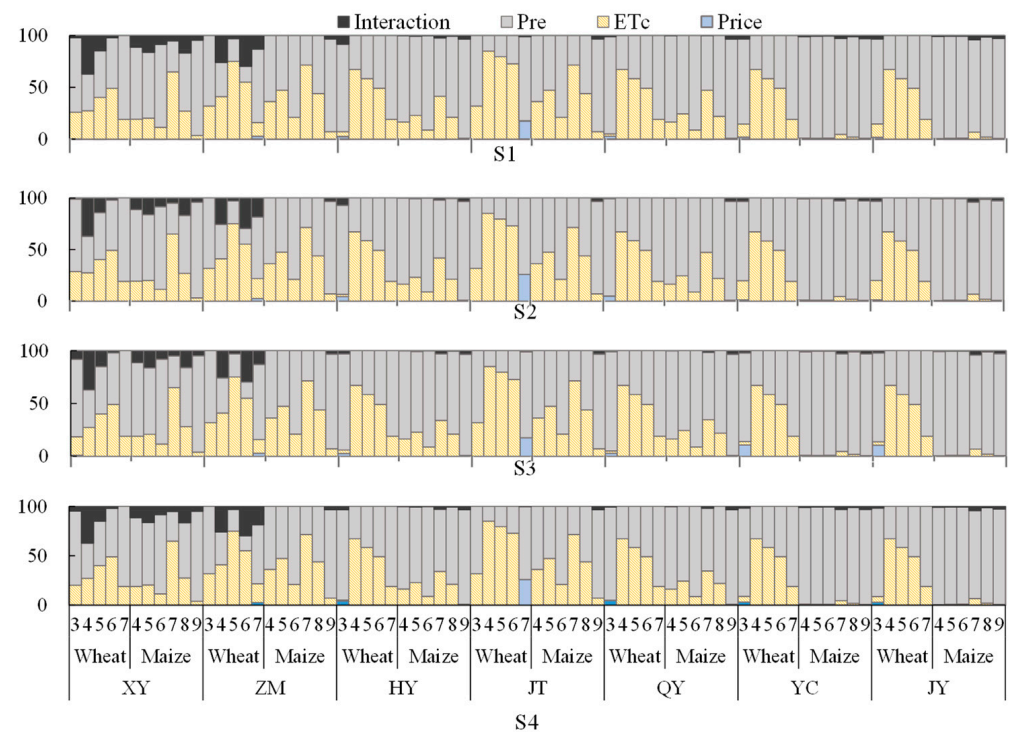


Figure 10. The contribution of variable uncertainty to variation in optimized irrigation schemes. The contribution of precipitation (Pre), crop evapotranspiration (ETc), crop prices, and their interactions are in grey, yellow, blue, and black, respectively. S1 to S4 are the four price scenarios, representing low-price wheat-low-price maize (S1), high-price wheat-low-price maize (S2), low-price wheat-high-price maize (S3), and high-price wheat-high-price maize (S4).

Divergent findings appear in terms of the variables influencing variation in the optimized system's net benefits. Price uncertainty emerges as the most influential factor, followed by precipitation, then crop evapotranspiration, with their interaction being the least significant. Crop price uncertainty contributes the most to variation in system net benefits: 57%, 47%, 39%, and 54% across scenarios 1 to 4. Uncertainty in precipitation contributes 26%, 33%, 37%, and 29% and uncertainty in crop evapotranspiration contributes 17%, 21%, 24%, and 19% in the four scenarios, respectively. The contributions of the interaction term to the objective's uncertainty are negligible, all less than 0.2% in the four scenarios. Crop evapotranspiration and precipitation affect crop yield through the

Jensen water production function, and the price is directly multiplied by crop yield and then affects benefits.

Overall, uncertainties in precipitation and crop evapotranspiration are the main sources of uncertainty in optimized irrigation schemes, which is consistent with research conducted in the Heihe river basin [47,48]. Although crop prices minimally affect water allocation schemes, decision-makers must remain vigilant as they profoundly influence the farmers' benefits by directly multiplying crop yield.

4.3. Risk Evaluation of Irrigation Water Shortages

To assess the water shortage risk for wheat and maize across various irrigation areas in Liangzhou County, this study used the proposed cloud-model-based integrated evaluation method. Employing 1000 groups of irrigation schemes obtained through the optimization model, the values for five risk factors were calculated. Figure 11 illustrates the classification clouds of the five risk factors for each level, while Figure 12 presents the integrated risk evaluation results for wheat and maize in each district.

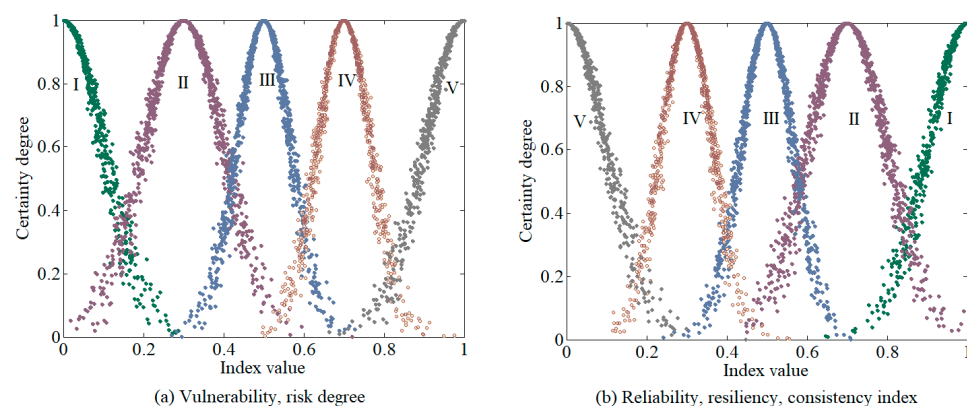


Figure 11. Classification clouds of evaluation levels I to V for each factor: reliability, vulnerability, resiliency, consistency index, and risk degree.

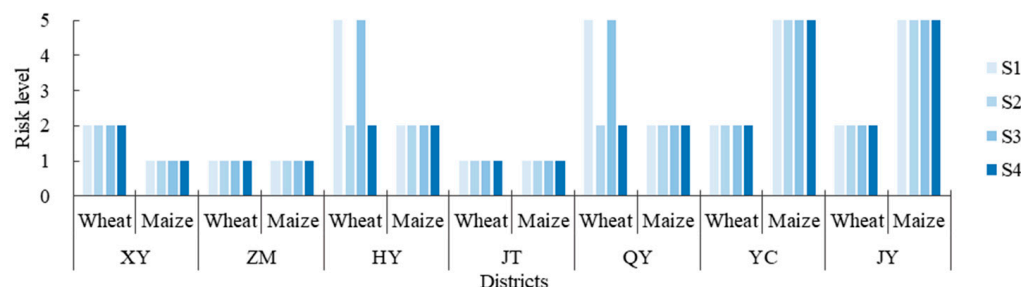


Figure 12. Irrigation water shortage risk evaluation results. The ordinates 1, 2, 3, 4, and 5 in the figure represent water shortage risk levels I, II, III, IV, and V, respectively. S1 to S4 are four price scenarios, representing low-price wheat–low-price maize (S1), high-price wheat–low-price maize (S2), low-price wheat–high-price maize (S3), and high-price wheat–high-price maize (S4).

Given that the evaluated irrigation schemes have undergone optimization, water shortage risks for most cases fall within the low or lower middle risk levels. This includes maize and wheat in the XY, ZM, and JT areas, maize in the HY and QY areas, and wheat in the YC and JT areas. Notably, ZM and JT, benefiting from ample water resources, exhibit the lowest water shortage risk. However, maize in the YC and JY districts faces a high irrigation shortage risk, primarily driven by high risk levels in reliability and resiliency.

Except for wheat in HY and QY, irrigation shortage risk levels remain consistent across all four scenarios. The aforementioned exceptions exhibit lower middle risk levels in scenarios 2 and 4, but the shift to high risk levels in scenarios 1 and 3. Upon revisiting the allocation schemes, it was observed that water allocation in March for wheat in low-price

scenarios tends to be lower than in high-price scenarios, averaging 19% and 21% for HY and QY, respectively. This reduction leads to an escalation in comprehensive risk levels, particularly to a high level.

While incorporating multiple uncertainties enhances the realism of the optimization model, the resulting broad range of optimized water allocation schemes may confuse decision-makers when selecting from among the schemes. It is essential to emphasize that the framework proposed in this study represents and describes uncertainty without actively reducing it. A potential way for narrowing the boundaries of uncertain variables is integrating reliable forecasting methods into the optimization model. Predicting uncertain variables more accurately could reduce the variability in their values. Subsequently, uncertainty representations like the cloud model could be applied to describe the remaining uncertainty in a more refined manner. Although this approach presents a feasible idea for narrowing the boundaries of water allocation schemes, it requires further research and in-depth discussion.

5. Conclusions

A cloud-based framework was proposed for precision agriculture to optimize scarce water resources in arid environments amid uncertainty. The case study results illustrate the cloud model's efficacy in representing the vagueness inherent in human thinking. The study enhances our understanding of how uncertainties impact the allocation of scarce water resources. Crop prices emerge as the most significant contributor to the variance in system benefits, while precipitation and evapotranspiration are the primary sources of uncertainty in water allocation schemes. The comprehensive assessment of irrigation shortage risks indicates that most districts exhibit low or relatively low risk levels, with exceptions noted for maize in the YC and JY districts, urging heightened attention to these areas.

The framework proposed in this study represents and describes uncertainty instead of actively reducing it. A potential way to narrow the boundaries of uncertain variables is by integrating reliable forecasting methods into the optimization model, such as better forecasting precipitation and evapotranspiration.

Supplementary Materials: The following supporting information can be downloaded at: <https://www.mdpi.com/article/10.3390/agronomy14010045/s1>, Figure S1: Meteorological data; Figure S2: Empirical and simulated stochastic distributions of precipitation, crop evapotranspiration for maize, and crop evapotranspiration for wheat.

Author Contributions: Conceptualization, F.Z. and B.S.; methodology, B.S.; software, F.Z., P.T. and T.Z.; validation, J.L. and F.L.; formal analysis, F.Z.; investigation, F.Z.; data collection and analysis: P.T.; data interpretation: J.L.; writing—original draft preparation, F.Z., P.T. and F.L.; writing—review and editing, B.S.; visualization, J.L.; supervision, B.S.; funding acquisition, F.Z. All authors have read and agreed to the published version of the manuscript.

Funding: This research was funded by the Fundamental Research Funds for the Central Universities, Grant No. BLX202212 and QNTD202303; Yinshanbeilu Grassland Eco-hydrology National Observation and Research Station, China Institute of Water Resources and Hydropower Research, Beijing 100038, China, Grant No. YSS202315.

Data Availability Statement: Data available on request.

Acknowledgments: We would like to express our memory of Ping Guo, and our gratitude to Hao Li for the discussions. We would like to extend our appreciation to anonymous reviewers and editors for their comments and suggestions that are significantly helpful in improving the quality of this paper.

Conflicts of Interest: The authors declare no conflicts of interest.

Appendix A. The Introduction of the Cloud Model

The cloud model is a method for transforming uncertainty between qualitative concepts and their quantitative expressions [37]. It was first proposed by Li et al. [31], and a brief introduction of its concept is detailed as follows.

If U is a quantity domain described with accurate numbers and C is the qualitative concept in U . If the quantity value, $x \in U$ and x randomly realizes the concept C , $\mu(x)$ is the certainty degree (membership degree) of x to C , $\mu(x) \in [0, 1]$, it is the random number which has a steady tendency [37]:

$$\mu : U \rightarrow [0, 1] \quad \forall x \in U \quad x \rightarrow \mu(x) \quad (\text{A1})$$

Then, the distribution of x on C is defined as a cloud, and each x is called a cloud drop. There are three numerical characteristics for a cloud: the expected value Ex , the entropy En (the uncertainty measurement of the qualitative concept), and the hyper entropy He (the uncertainty measurement of the entropy) for reflecting the whole characteristics of the qualitative concept.

Due to the wide-ranging existence of normal distributions in the real world, the normal cloud is the most popular cloud model among floating cloud, geometry cloud, and other cloud types. If U is a universal set described by precise numbers and C is the qualitative concept related to U , there is a number $x \in U$, which is a random realization of the concept C . If x satisfies $x \sim N(Ex, En'^2)$, where $En' \sim N(En, He^2)$, and the certainty degree of x on C is $\mu = \exp\left[-(x - Ex)^2 / (2(En')^2)\right]$, then the distribution of x on U is a normal cloud [49].

The forward cloud generator is a mapping process from qualitative concepts to quantitative data, while the backward cloud generator is the opposite. The algorithms of the forward generator and backward generators are shown in Appendices B and C, respectively.

Appendix B. The Forward Cloud Generator

A forward cloud generator is a mapping process from quality to quantity, generating cloud drops according to Ex , En , and He . The forward normal cloud generator algorithm is as follows [31]:

Input: (Ex, En, He) and the number of cloud drops n ;

Output: n of cloud drops x and their certainty degree μ , i.e., Drop (x_i, μ_i) , $i = 1, 2, \dots, n$;
Steps:

1. Generate a normally distributed random number En'_i with expectation En and variance He^2 , i.e., $En'_i = \text{NORM}(En, He^2)$;
2. Generate a normally distributed random number x_i with expectation Ex and variance En'_i , i.e., $x_i = \text{NORM}(Ex, En'_i)$;
3. Calculate $\mu_i = \exp\left(-\frac{(x_i - Ex)^2}{2(En'_i)^2}\right)$;
4. x_i with certainty degree of μ_i is a cloud drop in the domain;
5. Repeat steps 1–4 until n cloud drops are generated.

There are two special cases: if $He = 0$, step 1 will always provide an invariable number En , so x will become a normal distribution; if $He = 0$, $En = 0$, the generated x will be a constant Ex and $\mu = 1$.

Appendix C. Two Backward Normal Cloud Generators

A backward cloud generator is the inverse operation of a forward normal generator. It can realize the transformation from quantitative data to qualitative concepts, expressed in Ex , En , and He . In real situations, there are two cases for constructing a cloud model from known information; that is, the known information is a data series or boundary. So, two types of backward cloud generators exist accordingly.

For case 1, given a data series $X = \{x_1, x_2, \dots, x_d\}$ of length d , a cloud model could be constructed to extract the distribution characteristic of the series [50], described by Equation (A2).

$$\begin{cases} Ex = \frac{1}{d} \sum_{i=1}^d x_i \\ En = \sqrt{\frac{\pi}{2} \cdot \frac{1}{d} \cdot \sum_{i=1}^d |x_i - Ex|} \\ He = \sqrt{\frac{1}{d-1} \sum_{i=1}^d (x_i - Ex)^2 - En^2} \end{cases} \quad (\text{A2})$$

For case 2, given a bilateral boundary of the form B (B_{\min}, B_{\max}), three parameters (Ex , En , He) can be determined by Equation (A3).

$$\begin{cases} Ex = (B_{\min} + B_{\max})/2 \\ En = (B_{\max} - B_{\min})/6 \\ He = k \cdot En \end{cases} \quad (\text{A3})$$

where k is a constant and can be adjusted according to the fuzzy threshold of the variable, often taking 0.1 [51]. For a single boundary, such as B_1 ($-\infty, B_{1\max}$) or B_2 ($B_{2\min}, +\infty$), the expected value of the default boundary can be determined according to the upper or lower limit of the actual problem and then calculating by Equation (A3).

References

- Ickowitz, A.; Powell, B.; Rowland, D.; Jones, A.; Sunderland, T. Agricultural intensification, dietary diversity, and markets in the global food security narrative. *Glob. Food Secur.* **2019**, *20*, 9–16. [[CrossRef](#)]
- Tilman, D.; Balzer, C.; Hill, J.; Befort, B.L. Global food demand and the sustainable intensification of agriculture. *Proc. Natl. Acad. Sci. USA* **2011**, *108*, 20260–20264. [[CrossRef](#)] [[PubMed](#)]
- van Dijk, M.; Morley, T.; Rau, M.L.; Saghai, Y. A meta-analysis of projected global food demand and population at risk of hunger for the period 2010–2050. *Nat. Food* **2021**, *2*, 494–501. [[CrossRef](#)] [[PubMed](#)]
- Fernández-Cirelli, A.; Arumí, J.L.; Rivera, D.; Boochs, P.W. Environmental effects of irrigation in arid and semi-arid Regions. *Chil. J. Agr. Res.* **2009**, *69*, 27–40. [[CrossRef](#)]
- Schmitt, R.J.P.; Rosa, L.; Daily, G.C. Global expansion of sustainable irrigation limited by water storage. *Proc. Natl. Acad. Sci. USA* **2022**, *119*, e2214291119. [[CrossRef](#)] [[PubMed](#)]
- Smolenaars, W.J.; Sommerauer, W.J.W.; van der Bolt, B.; Jamil, M.K.; Dhaubanjar, S.; Lutz, A.; Immerzeel, W.; Ludwig, F.; Biemans, H. Spatial adaptation pathways to reconcile future water and food security in the Indus River basin. *Commun. Earth Environ.* **2023**, *4*, 410. [[CrossRef](#)]
- Rosa, L.; Chiarelli, D.D.; Rulli, M.C.; Dell’Angelo, J.; D’Odorico, P. Global agricultural economic water scarcity. *Sci. Adv.* **2020**, *6*, eaaz6031. [[CrossRef](#)]
- Hanjra, M.A.; Ferede, T.; Gutta, D.G. Pathways to breaking the poverty trap in Ethiopia: Investments in agricultural water, education, and markets. *Agric. Water Manag.* **2009**, *96*, 1596–1604. [[CrossRef](#)]
- Antonelli, M.; Gilmont, M.; Roson, R. Water’s Green Economy: Alternative Pathways for Water Resource Development in Agriculture. *L’Europe En Forme.* **2013**, *365*, 23–47. [[CrossRef](#)]
- Li, M.; Li, J.; Singh, V.P.; Fu, Q.; Liu, D.; Yang, G. Efficient allocation of agricultural land and water resources for soil environment protection using a mixed optimization-simulation approach under uncertainty. *Geoderma* **2019**, *353*, 55–69. [[CrossRef](#)]
- Bekri, E.; Disse, M.; Yannopoulos, P. Optimizing water allocation under uncertain system conditions for water and agriculture future scenarios in Alfeios River Basin (Greece)—Part B: Fuzzy-boundary intervals combined with multi-stage stochastic programming model. *Water* **2015**, *7*, 6427–6466. [[CrossRef](#)]
- Cunha, M.D. Water and environmental systems management under uncertainty: From scenario construction to robust solutions and adaptation. *Water Resour. Manag.* **2023**, *37*, 2271–2285. [[CrossRef](#)]
- Loucks, D.P.; van Beek, E. *Water Resource Systems Planning and Management*; Springer: Berlin/Heidelberg, Germany, 2017. [[CrossRef](#)]
- Sahoo, B.; Lohani, A.K.; Sahu, R.K. Fuzzy Multiobjective and Linear Programming Based Management Models for Optimal Land-Water-Crop System Planning. *Water Resour. Manag.* **2006**, *20*, 931–948. [[CrossRef](#)]
- Singh, S.K.; Yadav, S.P. Modeling and optimization of multi objective non-linear programming problem in intuitionistic fuzzy environment. *Appl. Math. Model.* **2015**, *39*, 4617–4629. [[CrossRef](#)]
- Alizadeh, M.R.; Nikoo, M.R.; Rakhshandehroo, G.R. Hydro-environmental management of groundwater resources: A fuzzy-based multi-objective compromise approach. *J. Hydrol.* **2017**, *551*, 540–554. [[CrossRef](#)]
- Xie, Y.L.; Xia, D.X.; Ji, L.; Huang, G.H. An inexact stochastic-fuzzy optimization model for agricultural water allocation and land resources utilization management under considering effective rainfall. *Ecol. Indic.* **2018**, *92*, 301–311. [[CrossRef](#)]

18. Russell, S.O.; Campbell, P.F. Reservoir operating rules with fuzzy programming. *J. Water Resour. Plan. Manag.* **1996**, *122*, 165–170. [[CrossRef](#)]
19. Ma, X.; Wang, H.; Yu, L.; Li, Y.; Fan, Y.; Zhang, J.; Zhang, J. Multi-preference based interval fuzzy-credibility optimization for planning the management of multiple water resources with multiple water-receiving cities under uncertainty. *J. Hydrol.* **2020**, *591*, 125259. [[CrossRef](#)]
20. Wang, B.; Cai, Y.; Yin, X.A.; Tan, Q.; Hao, Y. An integrated approach of system dynamics, orthogonal experimental design and inexact optimization for supporting water resources management under uncertainty. *Water Resour. Manag.* **2017**, *31*, 1665–1694. [[CrossRef](#)]
21. Zhang, F.; Cui, N.; Guo, S.; Yue, Q.; Jiang, S.; Zhu, B.; Yu, X. Irrigation strategy optimization in irrigation districts with seasonal agricultural drought in southwest China: A copula-based stochastic multiobjective approach. *Agric. Water Manag.* **2023**, *282*, 108293. [[CrossRef](#)]
22. Yue, Q.; Zhang, F.; Zhang, C.; Zhu, H.; Tang, Y.; Guo, P. A full fuzzy-interval credibility-constrained nonlinear programming approach for irrigation water allocation under uncertainty. *Agric. Water Manag.* **2020**, *230*, 105961. [[CrossRef](#)]
23. Shan, B.Y.; Guo, S.S.; Wang, Y.Z.; Li, H.; Guo, P. Vine copula and cloud model-based programming approach for agricultural water allocation under uncertainty. *Stoch. Environ. Res. Risk Assess.* **2021**, *35*, 1895–1915. [[CrossRef](#)]
24. Mahjouri, N.; Abbasi, M.R. Waste load allocation in rivers under uncertainty: Application of social choice procedures. *Environ. Monit. Assess.* **2015**, *187*, 5. [[CrossRef](#)]
25. Zhang, C.; Guo, P. FLFP: A fuzzy linear fractional programming approach with double-sided fuzziness for optimal irrigation water allocation. *Agric. Water Manag.* **2018**, *199*, 105–119. [[CrossRef](#)]
26. Zadeh, L.A. The concept of a linguistic variable and its application to approximate reasoning—I. *Inf. Sci.* **1975**, *8*, 199–249. [[CrossRef](#)]
27. Zadeh, L.A. Fuzzy sets. *Inf. Control* **1965**, *8*, 338–353. [[CrossRef](#)]
28. Li, D.; Liu, C.; Gan, W. A new cognitive model: Cloud model. *Int. J. Intell. Syst.* **2009**, *24*, 357–375. [[CrossRef](#)]
29. Lu, H.; Ren, L.; Chen, Y.; Tian, P.; Liu, J. A cloud model based multi-attribute decision making approach for selection and evaluation of groundwater management schemes. *J. Hydrol.* **2017**, *555*, 881–893. [[CrossRef](#)]
30. Zhang, S.; Xiang, M.; Xu, Z.; Wang, L.; Zhang, C. Evaluation of water cycle health status based on a cloud model. *J. Clean. Prod.* **2020**, *245*, 118850. [[CrossRef](#)]
31. Li, D.; Meng, H.; Shi, X. Membership clouds and membership cloud generators. *J. Comput. Res. Dev.* **1995**, *32*, 15–20.
32. Liao, Y.J.; Zhao, H.T.; Jiang, Y.; Ma, Y.K.; Luo, X.; Li, X.Y. An innovative method based on cloud model learning to identify high-risk pollution intervals of storm-flow on an urban catchment scale. *Water Res.* **2019**, *165*, 115007. [[CrossRef](#)]
33. Xu, J.; Ding, R.; Li, M.; Dai, T.; Zheng, M.; Yu, T.; Sui, Y. A new Bayesian network model for risk assessment based on cloud model, interval type-2 fuzzy sets and improved D-S evidence theory. *Inf. Sci.* **2022**, *618*, 336–355. [[CrossRef](#)]
34. Liu, P.; Liu, X. Multi-attribute group decision-making method based on cloud distance operators with linguistic information. *Int. J. Fuzzy Syst.* **2016**, *19*, 1011–1024. [[CrossRef](#)]
35. Yang, X.; Yan, L.; Peng, H.; Gao, X. Encoding words into Cloud models from interval-valued data via fuzzy statistics and membership function fitting. *Knowl.-Based Syst.* **2014**, *55*, 114–124. [[CrossRef](#)]
36. Deng, W.; Wang, G. A novel water quality data analysis framework based on time-series data mining. *J. Environ. Manag.* **2017**, *196*, 365–375. [[CrossRef](#)]
37. Gao, Y. An optimization algorithm based on cloud model. In Proceedings of the 2009 International Conference on Computational Intelligence and Security, Beijing, China, 11–14 December 2009; pp. 84–87.
38. Jensen, M.E. Water consumption by agricultural plants. In *Plant Water Consumption and Response; Water Deficits and Plant Growth*; Kozlowski, T.T., Ed.; Academic Press: New York, NY, USA, 1968; Volume II, pp. 1–22.
39. Kang, S.; Cai, H. *Agricultural Water Management*; China Agriculture Press: Beijing, China, 1996.
40. Li, M.; Guo, P.; Singh, V.P.; Yang, G. An uncertainty-based framework for agricultural water-land resources allocation and risk evaluation. *Agric. Water Manag.* **2016**, *177*, 10–23. [[CrossRef](#)]
41. Déqué, M.; Rowell, D.P.; Lüthi, D.; Giorgi, F.; Christensen, J.H.; Rockel, B.; Jacob, D.; Kjellström, E.; de Castro, M.; van den Hurk, B. An intercomparison of regional climate simulations for Europe: Assessing uncertainties in model projections. *Clim. Chang.* **2007**, *81*, 53–70. [[CrossRef](#)]
42. Bosshard, T.; Carambia, M.; Goergen, K.; Kotlarski, S.; Krahe, P.; Zappa, M.; Schär, C. Quantifying uncertainty sources in an ensemble of hydrological climate-impact projections. *Water Resour. Res.* **2013**, *49*, 1523–1536. [[CrossRef](#)]
43. Gu, W.; Shao, D.; Jiang, Y. Risk evaluation of water shortage in source area of Middle Route Project for South-to-North Water Transfer in China. *Water Resour. Manag.* **2012**, *26*, 3479–3493. [[CrossRef](#)]
44. Hashimoto, T.; Stedinger, J.R.; Loucks, D.P. Reliability, resiliency, and vulnerability criteria for water resource system performance evaluation. *Water Resour. Res.* **1982**, *18*, 14–20. [[CrossRef](#)]
45. Allen, R.G.; Pereira, L.S.; Raes, D.; Smith, M. *Crop Evapotranspiration-Guidelines for Computing Crop Water Requirements-FAO Irrigation and Drainage Paper 56*; FAO: Rome, Italy, 1998; p. 327.
46. Zhang, L.; Guo, P.; Fang, S.; Li, M. Monthly optimal reservoirs operation for multicrop deficit irrigation under fuzzy stochastic uncertainties. *J. Appl. Math.* **2014**, *2014*, 105391. [[CrossRef](#)]

47. Li, M.; Fu, Q.; Singh, V.P.; Ma, M.; Liu, X. An intuitionistic fuzzy multi-objective non-linear programming model for sustainable irrigation water allocation under the combination of dry and wet conditions. *J. Hydrol.* **2017**, *555*, 80–94. [[CrossRef](#)]
48. Zhang, F.; Zhang, C.; Yan, Z.; Guo, S.; Wang, Y.; Guo, P. An interval nonlinear multiobjective programming model with fuzzy-interval credibility constraint for crop monthly water allocation. *Agric. Water Manag.* **2018**, *209*, 123–133. [[CrossRef](#)]
49. Li, D.; Wang, S.; Li, D. *Spatial Data Mining: Theory and Application*; Springer: Berlin/Heidelberg, Germany, 2015. [[CrossRef](#)]
50. Liu, C.; Feng, M.; Dai, X.; Li, D. A new algorithm of backward cloud. *J. Syst. Simul.* **2004**, *16*, 2417–2420. [[CrossRef](#)]
51. Liu, D.; Wang, D.; Wu, J.; Wang, Y.; Wang, L.; Zou, X.; Chen, Y.; Chen, X. A risk assessment method based on RBF artificial neural network—Cloud model for urban water hazard. *J. Intell. Fuzzy Syst.* **2014**, *27*, 2409–2416. [[CrossRef](#)]

Disclaimer/Publisher’s Note: The statements, opinions and data contained in all publications are solely those of the individual author(s) and contributor(s) and not of MDPI and/or the editor(s). MDPI and/or the editor(s) disclaim responsibility for any injury to people or property resulting from any ideas, methods, instructions or products referred to in the content.